

## Evidence for unconventional superconductivity in $\text{UPt}_3$ from magnetic torque studies

Stephan Schöttl and Erwin A. Schubert

*Walther-Meissner-Institut für Tieftemperaturforschung, Walther-Meissner-Straße 8, D-85748 Garching, Germany*

Karol Flachbart

*Institute of Experimental Physics, SK-04353 Košice, Slovakia*

Jan B. Kycia and William P. Halperin

*Northwestern University, Evanston, Illinois 60208*

Alois A. Menovsky

*Van der Waals-Zeeman Laboratory, University of Amsterdam, Valckenierstraat 67, 1018 XE Amsterdam, The Netherlands*

E. Bucher and J. Hufnagl

*University of Konstanz, D-78457 Konstanz, Germany*

(Received 30 September 1998; revised manuscript received 13 December 1999)

We studied the anisotropic magnetic response of the internal superconducting phases of  $\text{UPt}_3$  and its anisotropic magnetic susceptibility with a capacitive torque meter which is very sensitive in high fields. Experiments were performed at temperatures down to 20 mK and at various angles between the  $c$  axis (hexagonal structure) and  $\vec{B}$ , ranging from  $16^\circ$  to  $82^\circ$ . The samples were four single crystals grown with different methods and subjected to different annealing procedures. The normal state susceptibility has a maximum around 20 K for  $\vec{B}$  in the  $a$ - $b$  plane which we followed up to 14 T. It may arise from hybridized uranium ion states split by the hexagonal crystal field. The magnetization curves in the superconducting (SC) regime show strong irreversibilities which are highly sample dependent. They are not correlated with the internal SC phase lines but continue up to a line of fields that lies parallel to the  $B_{c2}$  curve and even follows its kink at the tetracritical point  $(T^*, B^*)$ . In the cleanest sample this line is shifted to fields well below the  $B$ - $C$  internal phase line which then manifests itself in a pronounced kink of the magnetization curve indicating an enhanced Ginzburg-Landau parameter  $\kappa$ . In another sample the  $B$ - $C$  phase line between two of the three internal SC states could be detected even in the hysteretic region. The enhanced Ginzburg-Landau parameter  $\kappa$  means a larger penetration depth and/or a shorter coherence length, clear evidence for the unconventional character of the  $B$ - $C$  phase transition. With our cleanest sample we also observe an anomalous peak effect, a region of enhanced flux pinning near  $B_{c2}$ , which is probably related to the Fulde-Ferrell-Larkin-Ovchinnikov state. In yet another sample we find a crossing of the up-down magnetization curves, also near  $B_{c2}$ , but with reversed orientation of the magnetization loops. We interpret this in terms of different flux pinning in the two main crystal directions, possibly in relation to the peak effect which is, however, masked in this sample by strong irreversibilities.

### INTRODUCTION

Among the heavy Fermion systems  $\text{UPt}_3$  is the most widely studied compound because of its unusual superconducting (SC) properties. In low magnetic fields there is a double transition into the SC state,  $T_c^+$  and  $T_c^-$ , separated by about 60 mK, leading to phases denoted  $A$  and  $B$ , and there is another phase boundary to the so called  $C$  phase at higher fields. For all field orientations the internal phase lines meet in a tetracritical point, denoted  $(T^*, B^*)$ . Furthermore, the specific heat,<sup>1-3</sup> the penetration depth,<sup>4</sup> and the thermal conductivity<sup>5</sup> exhibit power laws in the SC region, instead of the usual activated behavior. The  $B$ - $C$  phase boundary has been established mostly by ultrasound velocity,<sup>6</sup> thermal expansion, and magnetostriction,<sup>7</sup> but so far no decisive signature in the magnetization has been reported.

Theoretical interpretations of this phase diagram suggest an unconventional SC order parameter with a symmetry lower than that of the Fermi surface. Under consideration are

either two symmetry unrelated one-dimensional components that lead to nearly degenerate  $T_c$ 's,<sup>8,9</sup> a one-dimensional order parameter combined with weak spin-orbit coupling,<sup>10</sup> or a single two-component order parameter belonging to a two-dimensional representation of the point group  $D_{6h}$  in which the degeneracy is lifted by a symmetry breaking field.<sup>11,12</sup> For the latter usually the weak antiferromagnetic ordering at 5 K is taken which was detected by neutron scattering, but also a structural texture, observed after annealing,<sup>13</sup> has been invoked.<sup>12</sup>

Recently, the focus of discussion has narrowed to the question if  $E_{1g}$  (Ref. 11) or  $E_{2u}$  (Ref. 12) is the relevant representation for the two-dimensional order parameter. Both have a line node at the equator (in the notation of a simplified spherical Fermi surface) and point nodes at the poles and differ only in the way the gap vanishes at the point nodes. For  $E_{1g}$  this is a linear function of  $k$ , whereas for  $E_{2u}$  the gap vanishes quadratically in  $k$ . Since the node structure is so similar, it is very difficult to distinguish experimentally be-

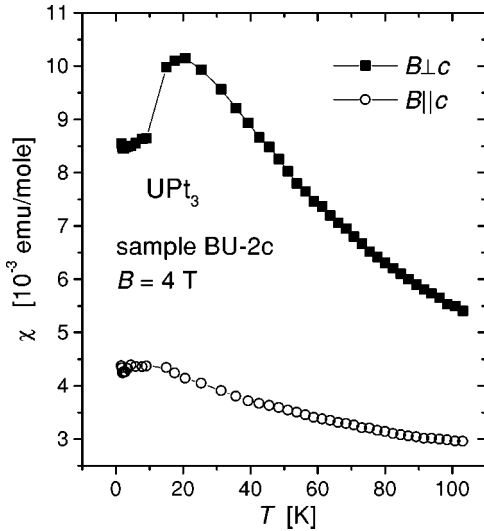


FIG. 1. Magnetic susceptibility of  $\text{UPt}_3$  for  $\vec{B}$  perpendicular and along the  $c$  axis of the single crystal No. 4c (BU-2c) measured in a vibrating sample magnetometer in 4 T.

tween both cases. The most recent experiments are studies on the thermal conductivity of  $\text{UPt}_3$  in low magnetic fields and at low temperatures.<sup>5</sup> They demonstrated again (through a scaling behavior in both variables) that the SC gap function should have lines of zeros, but they also could not resolve the issue of  $E_{1g}$  vs  $E_{2u}$ .

Another, more fundamental problem concerns the magnetic susceptibility and the nature of the heavy effective masses of  $\text{UPt}_3$  which are still not well understood. The usual one channel Kondo scenario is certainly not sufficient to provide an explanation. The biggest problem is the maximum around 20 K of the magnetic susceptibility  $\chi_{a,b}$ , i.e., with the external magnetic field  $\vec{B}$  in the crystallographic  $a$ - $b$  plane, see Fig. 1. To explain this maximum, the existence of antiferromagnetic fluctuations has been invoked,<sup>14</sup> but the data seem to be not decisive enough to explain the observed maximum quantitatively. Such maxima in known spin fluctuating systems such as Pd are usually very weak. Another possibility is the splitting of uranium  $5f$  levels in the hexagonal crystal field, as in the similar compound  $\text{PrNi}_5$  (Ref. 15) which shows a nearly identical temperature dependence of the susceptibility, both in  $a$ - $b$  plane and in the  $c$  direction. In contrast to this compound, in  $\text{UPt}_3$  the  $5f$  levels are hybridized with conduction band electrons and the effect of crystal field splitting needs a more detailed study. But the magnetism in  $\text{UPt}_3$  is even more complicated because of the existing anisotropy. A possible scenario which explains also the puzzling observation of a crossing of the upper critical field curves for  $\vec{B} \parallel \vec{c}$  and  $\vec{B} \parallel \vec{a}$  at 150–200 mK was proposed by Park and Joynt in 1996.<sup>11</sup> These authors assume a van Vleck-like susceptibility in the  $a$ - $b$  plane and a Pauli-like  $\chi_c$ . The first one would, similar to the case of  $\text{PrNi}_5$ , lead to a maximum of  $\chi_{a,b}$  due to level splitting in the hexagonal crystal field. But also in this model the origin of the heavy effective mass and the nature of the small ordered moments are unclear.

Our torque experiments in the normal phase were motivated by the fact, that for the proposed unconventional superconductor  $\text{UPt}_3$  a basic property such as the magnetic

susceptibility around 20 K is still not clarified. In addition to the normal phase anisotropic magnetic susceptibility we studied the anisotropic superconducting response to field and temperature variations. We used a capacitive torque meter which is very sensitive in high magnetic fields. The normal state torque is proportional to  $B^2$  and to the difference of the magnetic susceptibility  $\chi_{a,b} - \chi_c = \chi_{\text{aniso}}$  and a finite angle  $\Theta$  between the field and the crystallographic  $c$ -axis is required. In an anisotropic type-II superconductor a torque is generated by the fact that the shielding currents are no longer in a plane perpendicular to the field and  $\vec{m}(j_s) \parallel$  to  $\vec{B}$  creates a torque perpendicular to both  $\vec{m}$  and  $\vec{B}$ . Due to a small Meissner effect ( $\approx 2\%$ ),<sup>16,17</sup> in the case of  $\text{UPt}_3$  the SC torque is superimposed to a large background from vortices. One purpose of our experiment was to explore the three SC phases with a sensitive magnetic method. We found that the  $B$ - $C$  phase boundary manifests itself in a clear kink in the magnetization curves  $M_{\perp}(B)$  which points to an enhanced Ginzburg-Landau parameter  $\kappa$  in the  $C$  phase, which is clearly an unusual behavior.

## EXPERIMENTAL

Our capacitive torque meter is a modified version of that first introduced by Brooks *et al.*<sup>18</sup> The torque experienced in an external magnetic field (apart from shape effects which are negligible for  $\text{UPt}_3$  since  $\chi_{a,b,c}$  are small) is given by  $\tau = (1/\mu_0)\chi_{\text{aniso}}VB^2\cos\Theta\sin\Theta$ , where  $\chi_{\text{aniso}} = \chi_{a,b} - \chi_c$ ,  $\Theta$  is the angle between the anisotropy axis  $c$  and the external field, and  $\vec{\tau}$  is perpendicular to  $\vec{B}_{\text{ext}}$  and to  $\vec{c}$ .

For  $\text{UPt}_3$ , the anisotropy of the susceptibility which is sizable already at room temperature has been measured more than 14 years ago by Frings and Franse<sup>19</sup> and we confirmed these data with our sample BU-2c in a vibrating sample magnetometer in a field of 4 T, see Fig. 1.  $\chi_a$  and  $\chi_b$  are identical and show a maximum at 20.5 K, while  $\chi_c$  increases down to this temperature and then levels off. At the lowest temperatures  $\chi_a$  and  $\chi_b$  are about a factor of 2 larger than  $\chi_c$ , and we expected a strong torque even at mK temperatures.

The design of our torque meter is shown in Fig. 2. The upper capacitor plate with the narrow cantilever was etched out of OFHC copper. The dimensions of the ‘‘tongue’’ were  $0.05 \times 2.7 \times 0.4$  mm<sup>3</sup>.

*Samples.* The samples, all single crystals (depicted in Fig. 3), came from three different groups and were cut or cleaved off from larger parent crystals. One of them (sample No. 4) has already been investigated in a previous heat capacity experiment.<sup>20</sup> The first crystal (ME-2) was grown in Amsterdam with the Czochralski method and has been annealed for 24 h at 930°C. Two further samples (HA- $c$ -ax and HA- $a$ -ax,  $c$ -axis and  $a$ -axis oriented) were grown by the Northwestern group from electromigration purified uranium and they were tempered for 6 days at 800 and 970°C, respectively. They were cut out of a larger crystal by spark erosion. Both had excellent residual resistance ratios  $\rho_{300\text{ K}}/\rho_0$  of 892 (HA- $c$ -ax) and 957 (HA- $a$ -ax), respectively. The last sample (No. 4) was grown in Konstanz by electron beam melting from especially depleted uranium. Although it has not been annealed so far, we consider it an excellent sample judging from the high and sharp  $T_c$  (540 mK). After polishing the

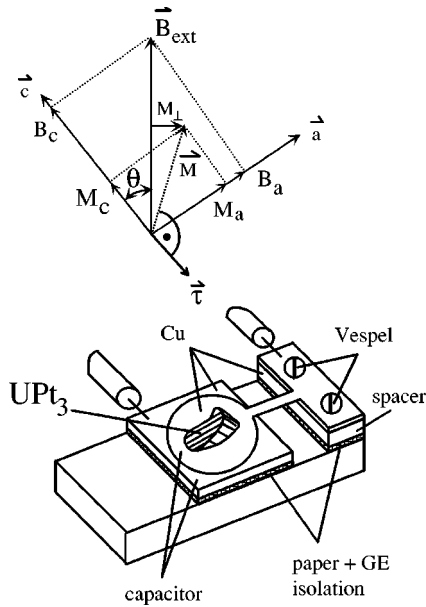


FIG. 2. Sketch of the capacitive torque meter used here. The cooling of the sample was provided through a thin lens paper soaked with GE varnish. The contact was good enough to cool the sample to temperatures below 20 mK.

surface for penetration depth measurements<sup>4</sup> it broke into three pieces, piece b was used here in the torque meter while piece c was investigated in the vibrating sample magnetometer.

**Thermometry.** The upper capacitor plate was electrically isolated from the body of the torque meter (OFHC copper or

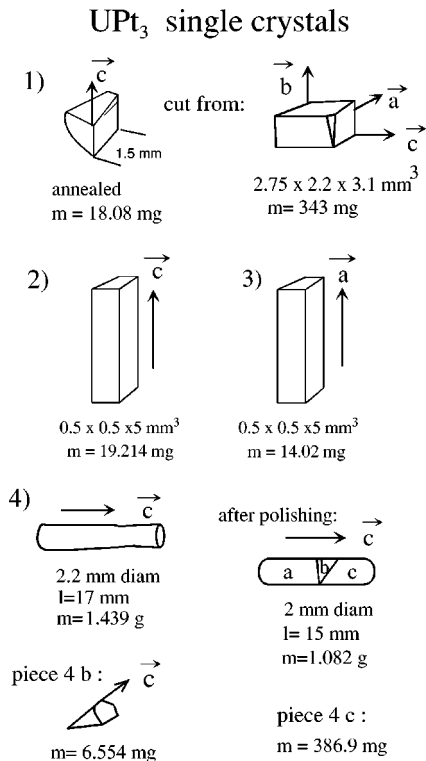


FIG. 3. Sketch of the samples used in this work. All samples are single crystals grown and annealed (except No. 4) in a different way, see text and Table I.

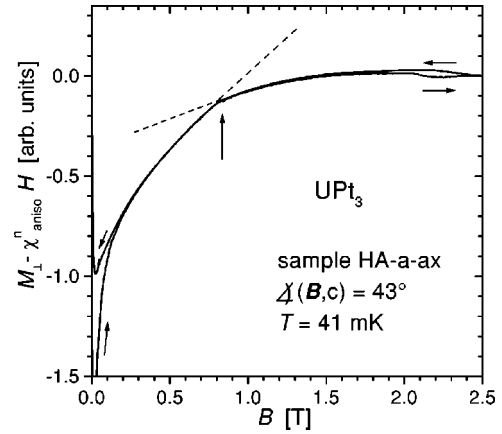


FIG. 4. Magnetization curve  $M_{\perp}(B)$  of sample No. 3. To obtain  $M_{\perp}(B)$ , the raw data  $\tau(B)$  was divided by  $B$ . In addition, for this plot the normal state contribution  $\chi_{\text{aniso}}^n H$  was subtracted. This sample had the highest residual resistance ratio and showed the smallest hysteresis.

Ag) by lens paper of 40  $\mu\text{m}$  thickness soaked with GE varnish. The latter was used to give good thermal contact to the plate onto which the samples were glued with DuPont silver epoxy. Estimates showed that the radioactive heat leak of the samples was low enough and the thermal contact through the GE varnish and the silver epoxy was good enough to cool the samples to below 20 mK with the body temperature below 10 mK provided by a dilution refrigerator. The temperatures of the sample holder were determined with a carbon resistor calibrated against NBS fix-point standards (in previous runs) and against a second carbon resistor in the field-compensated region of our cryostat when magnetic fields were applied.

The  $B$ - $T$  region between 0 and 7 T, 20 mK to 2 K was scanned by either sweeping the field at constant  $T$ , or by varying  $T$  in a constant field. Also slowly modulated sweeping fields (20–30 mHz ac fields with small amplitudes superimposed to the field ramp) were used.

Even at 20 mK the anisotropy was only about 10% less than at 4 K which demonstrates that  $\chi_{a,b}$  is still  $\approx 2\chi_c$  at this temperature. Since the SC internal phases differ in the order parameter and/or in the distribution or structure of the vortices we expected changes of  $\vec{\tau}$  at the phase boundaries, especially so since the torque is a very sensitive indicator of anisotropies.

## RESULTS

**$B$ - $C$  phase line.** In the superconducting phase the raw data  $\tau(B)$  at constant  $T$  were divided by  $B$  to obtain the magnetization curves for  $M_{\perp}(B)$ , the magnetization component perpendicular to  $\vec{B}$ . They were nearly reversible for sample No. 3, the  $a$ -oriented crystal with the highest residual resistance ratio. They display a kink around 0.8 T which flattens the curve (see Fig. 4) and thus points to an increased Ginzburg-Landau parameter  $\kappa$  in the  $C$  phase, which means a stronger type-II character of this phase. This behavior also leads to the well known kink of the  $B_{c2}$  curve above the tetracritical point. The reversibility of  $M_{\perp}(B)$  in the region where the kink occurs rules out the possibility that it could be due to changes in flux pinning. In the torque curve the

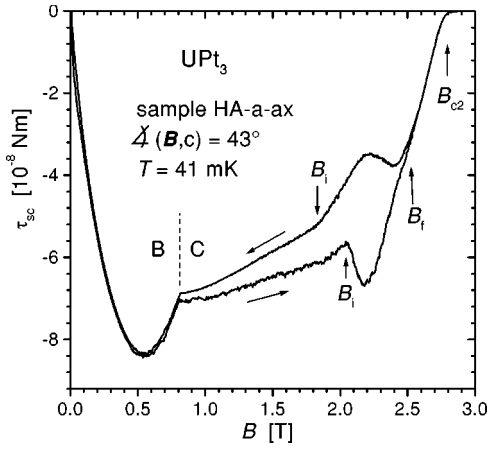


FIG. 5. Torque curves  $\vec{M} \times \vec{B}$  of sample No. 3 with the normal contribution  $\propto \chi_{\text{aniso}} B^2$  subtracted leaving the SC part  $\tau_{\text{SC}} \propto \vec{M}(j_s) \vec{B}$  which in an anisotropic superconductor stems from shielding currents in a plane which is not orthogonal to  $\vec{B}$ . The kink around 0.8 T marks the  $B$ - $C$  phase boundary. Between  $B_i$  and  $B_f$  an anomalous peak effect with hysteretic  $B_i$  is found.

kink is even more pronounced, see Fig. 5. The temperature dependence of the kink maps the  $B$ - $C$  phase transition, see Fig. 7. Its location under  $43^\circ$  is in accordance with the phase line found by Schenstrom *et al.*<sup>21</sup> under  $45^\circ$  which was close to the  $\vec{B}/\vec{a}$  phase line. The upper critical field was determined from the upper end of the curves in Fig. 5 and by the onset of the Meissner effect in field cooled  $T$  sweeps.

Our result is clear evidence for unconventional superconductivity. The possibility that at 0.8 T a magnetic phase transition takes place can be ruled out: above  $T_c$  we see no indication for such a transition and in this region a magnetic transition has never been observed in the literature. The only possibility which is left is a change in the Ginzburg-Landau parameter  $\kappa = \lambda/\xi$  of  $\text{UPt}_3$ . Either  $\lambda$  increases and/or  $\xi$  decreases. Both parameters depend on the mean free path in a way that the  $C$  phase would have to have a shorter one. In a scenario with a coupled SC and magnetic order parameter as discussed, e.g., by Blount *et al.*<sup>22</sup> one could speculate that, as in the  $C$  phase one component of the magnetic order parameter vanishes, more magnetic scattering centers exist, and as a consequence the mean free path would decrease. This would lead to the behavior we observed.

The kink in  $M_\perp$  was less pronounced with sample No. 2, due to a larger hysteresis, but it could still be discerned in the upward branch, see Fig. 6. It's position, though, is shifted to higher fields as compared to sample No. 3, most probably due to strong flux pinning. Therefore it does not lie at the right field value for the  $B$ - $C$  boundary but is still an indication of it. For both samples no transition could be detected above 400 mK (shaded area in Fig. 7), possibly because our method is less sensitive when  $B_{c2}$  is smaller at higher temperatures, or because the effect is smaller near  $T_c$ . From penetration depth measurements we know the temperature of the lower transition  $T_c^-$  in small fields<sup>16</sup> and the tentative location of the  $A$ - $B$  phase line is indicated in the figure.

*Anomalous peak effect.* Another remarkable feature in Fig. 5 is the irreversibility region near  $B_{c2}$  which is similar to the so-called peak effect in “dirty” type-II superconductors.

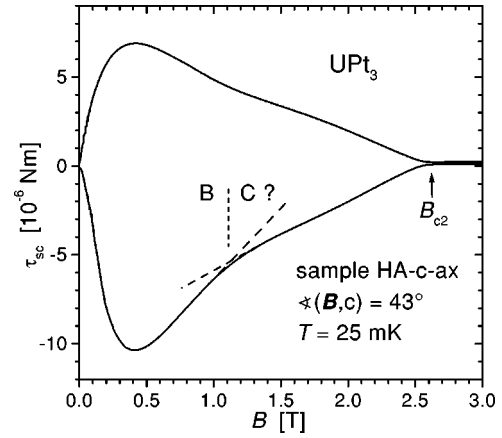


FIG. 6. Torque curves  $\vec{M} \times \vec{B}$  of sample No. 2. In spite of the larger hysteresis as compared to sample No. 3 a kink at the  $B$ - $C$  phase boundary is clearly seen, the peak effect is masked by the large irreversibilities. Note the difference in the scale as compared to Fig. 5.

In contrast to this we have here a system with a long mean free path for the electrons as compared to  $\xi_0$ . Such a “peak effect” for  $\text{UPt}_3$  has been found in Faraday magnetization measurements by Tenya *et al.*<sup>23</sup> and it was suspected to be the cause for a sharp drop of  $\chi''$  in ac susceptibility data just below  $T_c$ .<sup>24</sup> Its origin, however, could not be clarified in both cases. Our sample No. 3 is a rare exception among  $\text{UPt}_3$  probes for its widely reversible magnetization curve. This leads to a clear observation of the “peak effect” feature which is largely obscured by hysteresis in other samples, compare the scales in Figs. 5 and 6, or Tenya *et al.*<sup>23</sup>

A peak effect with exactly the same behavior as with our cleanest sample No. 3 was reported by Gegenwart *et al.*<sup>25</sup> for  $\text{UPd}_2\text{Al}_3$  and  $\text{CeRu}_2$ . In accordance with a theory by Tachiki *et al.*<sup>26</sup> it was interpreted as due to an anomalous Fulde-Ferrell-Larkin-Ovchinnikov state. Since we believe that in our case the same explanation is possible, we follow their argument here and we use the same notations. Between an onset field  $B_i$  which is hysteretic (first order phase transition?) and an offset field  $B_f$ , a region of strong flux pinning

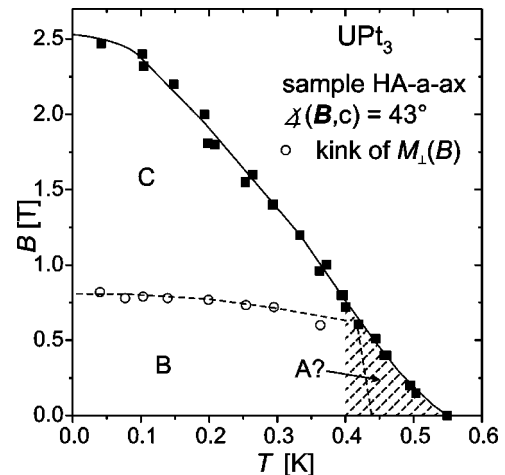


FIG. 7. Phase diagram showing the  $B$ - $C$  phase line as obtained from Fig. 5 (sample No. 3). In the shaded region no kink in  $M_\perp(B)$  could be detected. Full squares indicate  $B_{c2}$ .

TABLE I. Properties of the samples used in this work.  $RRR_c$  defines the residual resistance ratio along the  $c$  axis.

Sample	Mass (mg)	$\mu$ moles	$T_c^+$ (mK)	$T_c^-$ (mK)	Annealing temperature ( $^{\circ}$ C)	$RRR_c$
No. 1 ME-2	18.08	21.96	430	340	927, 24 h	
No. 2 HA- $c$ -ax	19.214	23.338	551	420	800, 6 days	892
No. 3 HA- $a$ -ax	14.020	17.029	549	not obs. in $\lambda$	970, 6 days	957
No. 4b BU-2b	6.554	7.961	540		not annealed	200
No. 4c BU-2c	386.9	469.94	540		not annealed	200

occurs due to the interaction of the Abrikosov vortices and a spatial modulation of the SC order parameter predicted by Fulde and Ferrell<sup>27</sup> in 1964 and by Larkin and Ovchinnikov<sup>27,28</sup> in 1965. For the Tachiki theory to apply the following conditions have to be met: (i) a large electronic mean free path  $l > \xi_0$ , (ii) Pauli limiting dominating over orbital pair breaking by the external magnetic field, (iii) a Zeeman energy density that equals the SC condensation energy density, and (iv) a short coherence length, or a large Ginzburg-Landau parameter  $\kappa$ . All of these requirements are fulfilled in  $UPt_3$ , and in fact this system was regarded as a further likely candidate to show the anomalous peak effect by Gegenwart *et al.* and Tachiki *et al.*<sup>25,26</sup> The coherence length is short (15 nm), the mean free path is long [ $l > 200$  nm estimated from the high residual resistance ratio value (see Table I)], Pauli limiting of the upper critical field is very likely the cause of the suppression of  $B_{c2}$  when  $\vec{B}$  is parallel to  $c$ , and the Zeeman energy density is even larger than the condensation energy.<sup>26</sup> For  $UPt_3$  the situation is, however, even more complicated than for the heavy Fermion systems investigated by Gegenwart *et al.* due to the internal SC phases, the anisotropic magnetic behavior, see below, and the stronger flux pinning already in the  $C$  phase.

*Anisotropic flux pinning.* For sample No. 1  $M_{\perp}(B)$  also showed large hysteretic regions throughout the SC phases, largest near  $B \approx 0$ , see Fig. 8.  $B_{c2}(T)$  was determined here by the disappearance of the hysteresis which defines an irreversibility line rather than  $B_{c2}$ , but the values obtained this way agreed very well with  $B_{c2}(T)$  from ultrasound attenuation measurements by Bruls *et al.*<sup>6</sup> on its parent crystal.

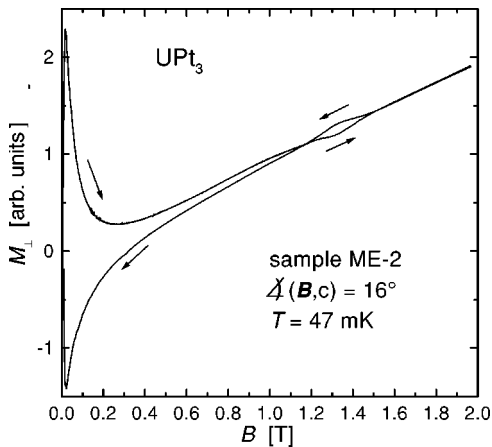


FIG. 8. Magnetization curve of  $UPt_3$ , sample No. 1. The raw data  $\tau(B)$  was divided by  $B$  to obtain  $M_{\perp}(B)$ .

Sample No. 1 showed a special peculiarity, see Fig. 8 and the enlarged example shown in Fig. 9: the magnetization curves cross at a certain field near  $B_{c2}(T)$  a behavior that is different from the peak effect where no crossing occurs and it is embedded in a region of strong irreversibilities. By reversing the field sweep direction loops with different orientations above and below the crossing point are formed. The ‘‘phase diagram’’ resulting from these  $B$  sweeps is shown in Fig. 10.

In  $T$  sweeps at constant field features corresponding to the peak effect and the crossing effect appeared, but were often masked by the strong flux pinning. These measurements were done either by cooling in the respective field from above  $T_c$  (Meissner curves), or by cooling in a different field (zero, higher, or lower) than the measuring field and warming through  $T_c$ . For the latter, large variations occurred in the peak effect region as in Fig. 11(a) and (b). These variations are due to the decay of nonequilibrium flux line configurations and shielding currents near  $T_c$ . Reversing the field sweep direction below  $T_c$  the opposite direction of the shielding currents led to a reversed torque signal. But also for Meissner curves strong irreversibilities due to strong flux pinning occurred, see Fig. 11. Cooling through  $T_c$  resulted in a small Meissner effect of  $\approx 2\%$  which means that most of the flux is prevented from being expelled in the peak effect region. Reversing the temperature sweep to warming resulted in the mentioned irreversibilities. After passing through a maximum and a minimum which depended on the field and temperature history of the sample, faster torque changes occurred above a temperature that corresponded to

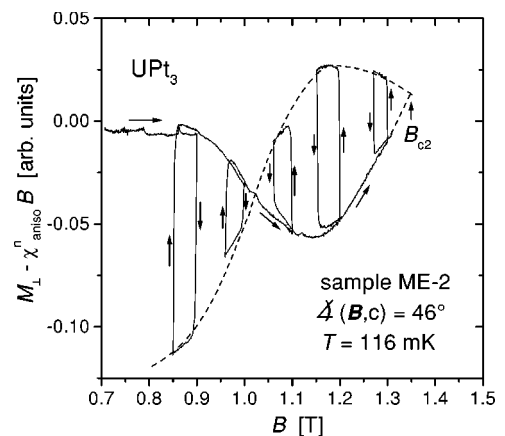


FIG. 9. Crossing of the up-down branches of the magnetization curve of  $UPt_3$ , sample No. 1. Each loop was obtained by stopping the field sweep at the upper and lower envelope [with no effect on  $M_{\perp}(B)$ ] and then reversing the sweep direction.

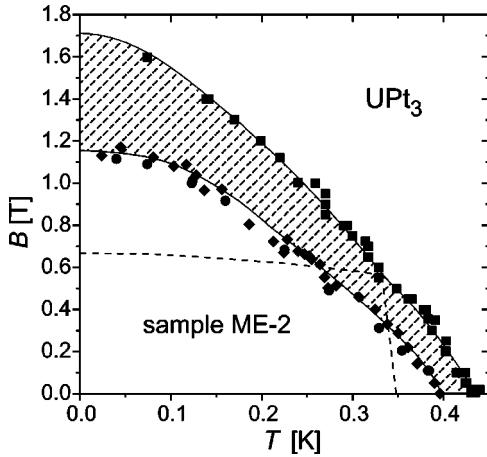


FIG. 10. Location of the crossing points in the  $B$ - $T$  plane derived from curves similar to those in Fig. 9. Full squares give  $B_{c2}$ , the full circles are from  $\Theta = 46^\circ$ , the full diamonds from  $\Theta = 16^\circ$  data. The dotted lines indicate the tentative internal SC phase lines.

the  $H_f$  field. Here the flux lines rearrange themselves more easily like in the case of the field sweep curves of Fig. 5. The position of the minima in the  $B$ - $T$  plane is shown in Fig. 12.

In a series of experiments we determined the dependence of the line of crossing points in the  $B$ - $T$  plane on the angle  $\Theta$  between  $\vec{B}$  and  $\vec{c}$ . At  $\Theta = 82^\circ$  the crossing line was indistin-

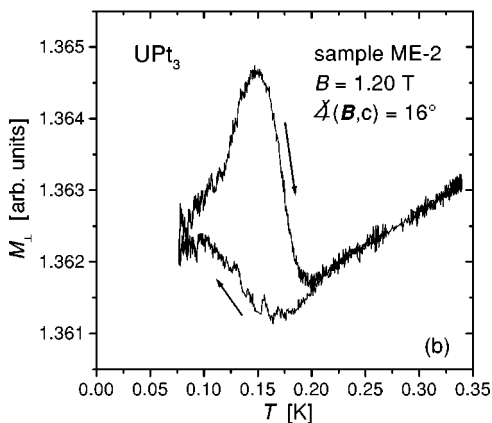
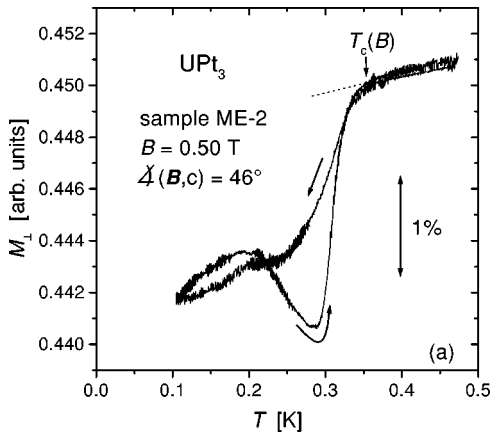


FIG. 11. (a) and (b) Irreversible part of the Meissner curve of  $\text{UPt}_3$  just below  $T_c$ , two examples. The torque changes are fastest between  $T_c$  and the minimum (a) or the maximum (b) of the upward branch of  $M_\perp(T)$ .

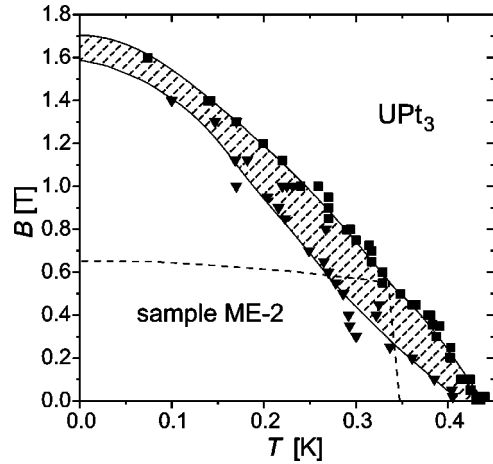


FIG. 12. Position of the minima (full triangles) of the upward Meissner curves  $M_\perp(T)$  of Fig. 11 in the  $B$ - $T$  plane. Full squares give  $B_{c2}$ , the dotted lines indicate the tentative internal SC phase lines.

guishable from  $B_{c2}(T)$ , otherwise no large variations with  $\Theta$  were found.

In Figures 10 and 12 no connection exists to the tetracritical point and to the internal SC phase lines. The crossing points and the  $B_f$ -boundary lines rather run along  $B_{c2}(T)$ , see the shaded areas in both figures.

*Normal state susceptibility.* Concerning the anisotropic normal state susceptibility of  $\text{UPt}_3$ , our data measured in a vibrating sample magnetometer in 4 T (Fig. 1) are practically identical to those of Frings and Franse<sup>19</sup> of 1985. Since  $\chi_c$  has only a slight variation around 20 K, the maximum in  $\chi_{a,b}$  is reflected in the torque vs  $T$  curves, see Fig. 13. We followed this torque maximum to higher fields (up to 14 T) and to zero field. After subtraction of the background signal from the empty torque meter the data are shown in Fig. 14. It can be seen that the maximum in  $\chi_{a,b}$  is suppressed by the magnetic field and probably tends to the metamagnetic transition at 20 T, 0 K which was found earlier.<sup>29</sup>

## DISCUSSION

The kink in the magnetization curves at the  $B$ - $C$  phase boundary (Figs. 5 and 6) is direct magnetic evidence for the

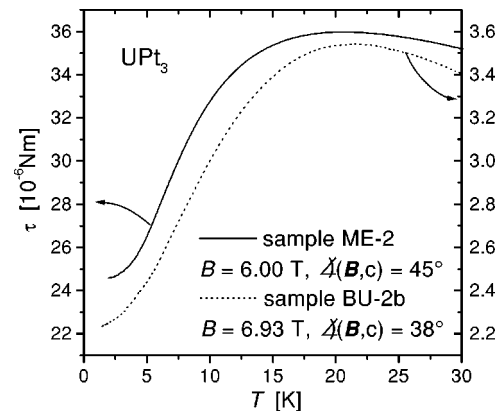


FIG. 13. Temperature dependence of  $\chi_{\text{aniso}}$  around 20 K. Note the absence of any feature at 5 K. The different scales for the two samples are due to different sample sizes, orientations, and the use of different cantilevers. They are otherwise consistent with  $\chi_{a,b} - \chi_c$  taken from Fig. 1

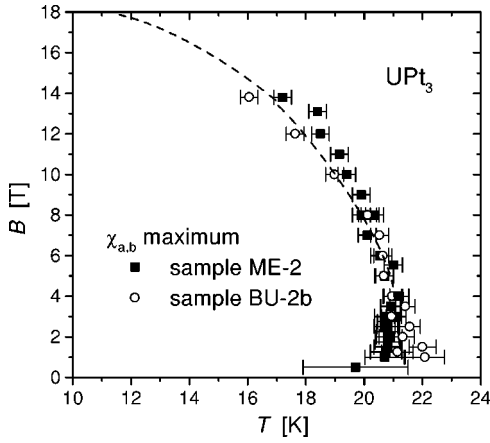


FIG. 14. Position of the maxima of  $\chi_{\text{aniso}}$  showing their field dependence. The error bars stem from the temperature variation during the field sweeps.

unconventional character of the internal SC phases of  $\text{UPt}_3$  and demonstrates the stronger type-II behavior of phase C. Previous theoretical papers dealt with the difference between the B and C phases, involving different flux line shapes (cross sections) and different configurations.<sup>8,9,30,31</sup> There is also experimental evidence for this from neutron scattering<sup>32</sup> interpreted theoretically by Joynt.<sup>33</sup> Different flux lines could indeed explain a kink in the magnetization curves and it remains to be determined which specific type would enhance  $\kappa$  in the way we observe it. Another possibility is the above mentioned disappearance of magnetic order in the C phase.

The best sample, No. 3, from Northwestern University with its widely reversible magnetization made it possible to distinguish the B-C phase line directly in magnetization on a two orders of magnitude finer scale than with other samples and with almost no hysteresis. The C phase is characterized by a stronger type-II behavior, most probably due to different flux line shapes and configurations.

Along the  $B_{c2}$  curve lies a region which shows an anomalous peak effect, different from the usual one in the fact that it occurs in a type-II superconductor which is in the clean limit. Our best sample allowed to observe it in a region with very small hysteresis. The possible connection of this effect to the Fulde-Ferrell-Larkin-Ovchinnikov state needs further investigation.

Another remarkable feature is the crossing of the magnetization curves of sample No. 1, occurring without a foregoing reversibility region. An explanation as in the case of the peak effect (strong flux pinning near  $B_{c2}$ ) is thus excluded. The crossing can be understood qualitatively in a model which invokes anisotropic, field and temperature dependent flux pinning, see Fig. 15. Let us neglect, for a moment, the normal state anisotropy and assume that the external magnetic field is oriented under  $45^\circ$  with respect to the  $c$  axis in the  $a$ - $c$  plane. In the region below the crossing line the pinning force along the  $a$  direction is now assumed to be larger than in the  $c$  direction. The result is, that during a field increase the  $a$  component of the magnetization is lagging behind its equilibrium value, farther than the  $c$  component. The magnetization thus lies left, above of the diagonal dashed line. At point A, as the sweep direction is reversed, the  $c$  component follows rapidly, the  $a$  component slowly and the

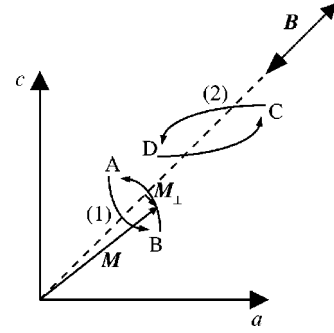


FIG. 15. Qualitative model to explain the different loop directions of the magnetization curves of Fig. 9 by anisotropic, field and temperature dependent irreversibilities. The external field  $\vec{B}$ , here assumed to be oriented in the diagonal of the  $a$ - $c$  plane, is generally swept upwards, but the sweep direction is changed to downwards at points A and C. As long as the normal state anisotropy is neglected, the equilibrium magnetization would vary along the dashed line. Because of strong flux pinning  $\vec{M}$  deviates from it and follows the loops (1) and (2). For loop (1) it is assumed that the flux pinning is stronger along the  $a$  direction than along  $c$ , while the contrary is taken for loop (2). As long as it lies above the diagonal the resulting torque is in the positive  $b$  direction (into the paper). The component  $M_{\perp}$ , as drawn here for the other case (lower right side of the dashed line) results in the negative  $b$  direction for the torque. Loop (1) is below, loop (2) above the crossing point field of Fig. 9. For further details, see text.

magnetization varies along branch (1) to point B. Then the field is raised again. After passing the crossing point, our model assumes that the pinning forces along the  $a$  and  $c$  direction change their relative magnitude. Thus, the magnetization vector goes to the right side of its equilibrium value. If the field sweep direction is again reversed at point C, the variation is reversed with respect to branch (1): the  $a$  component varies faster, the magnetization wanders to the left, to point D, where the sweep is again reversed until loop (2) closes at point C. The direction of the resulting torque is determined by the side (viewed from the direction of the external magnetic field) on which the pointer of the magnetization lies. If it is on the upper left,  $\vec{\tau}$  is in positive  $b$  direction, bottom right means negative  $b$  direction for  $\vec{\tau}$ . An example for the latter situation is drawn in Fig. 15 in the second branch of loop (1). As one can see, in both loops the magnetization changes its direction with respect to  $\vec{B}$  back and forth each time. In loop (1) this is from left to right and back, while in loop (2) the first change is from right to left. This explains the different orientations of the two loops. If one takes into account the anisotropy of the normal state, the equilibrium magnetization does no longer coincide with the direction of the external field which, however, still determines the position of the sign change of  $\vec{\tau}$  and the superconducting part of the torque still follows the loops described above.

This irreversible behavior depends strongly on crystal quality and is thus different in the different samples but is otherwise not connected to the internal phase boundaries. Similar features were detected with a Faraday magnetometer in other samples.<sup>23</sup>

In our opinion, the origin of the maximum in  $\chi_{a,b}$  around

20 K is not clarified. Arguing from a  $T^3 \ln T$  contribution to the heat capacity (in a small  $T$  range) Frings and Franse<sup>19</sup> and also Stewart<sup>34</sup> interpret the magnetic anisotropy as a signature of ferromagnetic spin fluctuations, but only antiferromagnetic fluctuations of very small magnetic moments ( $0.02\mu_B$ ) in the  $a$ - $b$  plane were found in neutron scattering<sup>35</sup> at 5 K. One plausible explanation for the magnetic behavior of  $\text{UPt}_3$  is that proposed by Park and Joynt<sup>11</sup> who assume a van Vleck type of enhanced magnetism in the  $a$ - $b$  plane (crystal field split excited magnetic states mix with the non-magnetic ground state) along with an slightly enhanced Pauli magnetism along the  $c$  axis. This model can also explain the crossing of the upper critical fields around 150 mK if  $B_{c2}(T)$  is Pauli limited in the  $c$  direction, but not along  $a$  or  $b$ . But even in this theory the exact nature of the hybridized, strongly correlated states which lead to the enhanced effective masses, is not exactly specified. Concerning the antiferromagnetic fluctuations below 5 K, we never detected any sign of it with our sensitive magnetic methods (SQUID mag-

netometry in low fields and torque in high fields). It was claimed that this might be due to the different time scales probed in static measurements and in neutron scattering.<sup>36</sup> This argument implies that the antiferromagnetic fluctuations are very weak on macroscopic time scales. Long range antiferromagnetic order developing out of these fluctuations<sup>36,37</sup> is most probably the cause of the increase of the specific heat below 50 mK and its maximum at 18 mK.<sup>3,38</sup> Detailed studies of the magnetism of  $\text{UPt}_3$  from above 20 K to below 50 mK are necessary to shed more light on its nature.

#### ACKNOWLEDGMENTS

We thank Dr. D. Einzel for fruitful discussions and we are grateful to Professor J. Brooks for communicating unpublished results on  $\text{UBe}_{13}$  which show similar properties in this compound. This work was supported by the DAAD and the NSF through Grant No. DMR-9705473.

- 
- <sup>1</sup>R. Fisher, S. Kim, B. Woodfield, N. Phillips, L. Taillefer, K. Hasselbach, J. Flouquet, A. Giorgi, and J.L. Smith, Phys. Rev. Lett. **62**, 1411 (1989).
- <sup>2</sup>K. Hasselbach, L. Taillefer, and J. Flouquet, Phys. Rev. Lett. **63**, 93 (1989).
- <sup>3</sup>E.A. Schuberth, B. Strickler, and K. Andres, Phys. Rev. Lett. **68**, 117 (1992).
- <sup>4</sup>F. Groß-Alltag, B.S. Chandrasekhar, D. Einzel, P.J. Hirschfeld, and K. Andres, Z. Phys. B: Condens. Matter **82**, 243 (1991).
- <sup>5</sup>H. Suderow, J.P. Brison, A. Huxley, and J. Flouquet, Phys. Rev. Lett. **80**, 165 (1998).
- <sup>6</sup>G. Bruls, D. Weber, B. Wolf, P. Thalmeier, B. Lüthi, A. deVisser, and A. Menovsky, Phys. Rev. Lett. **65**, 2294 (1990).
- <sup>7</sup>N.H. van Dijk, A. deVisser, J.J.M. Franse, and L. Taillefer, J. Low Temp. Phys. **93**, 101 (1993).
- <sup>8</sup>A. Garg and D. Chen, Phys. Rev. B **49**, 479 (1994).
- <sup>9</sup>M.E. Zhitomirsky and K. Ueda, Phys. Rev. B **53**, 6591 (1996).
- <sup>10</sup>K. Machida and M. Ozaki, Phys. Rev. Lett. **66**, 3293 (1991).
- <sup>11</sup>K.A. Park and R. Joynt, Phys. Rev. B **53**, 12 346 (1996).
- <sup>12</sup>J.A. Sauls, J. Low Temp. Phys. **95**, 153 (1994).
- <sup>13</sup>P.A. Midgeley, A. M. Hayden, L. Taillefer, B. Bogenberger, and H. v. Löhneysen, Phys. Rev. Lett. **70**, 678 (1993).
- <sup>14</sup>G. Aeppli, A. Goldman, G. Shirane, E. Bucher, and M.-Ch. Lux-Steiner, Phys. Rev. Lett. **58**, 808 (1987).
- <sup>15</sup>K. Andres, S. Darack, and H.R. Ott, Phys. Rev. B **19**, 5475 (1979).
- <sup>16</sup>S. Schöttl, E. A. Schuberth, K. Flachbart, J.B. Kycia, J.I. Hong, D.N. Seidman, W.P. Halperin, J. Hufnagl, and E. Bucher, Phys. Rev. Lett. **82**, 2378 (1999).
- <sup>17</sup>S. Wüchner, N. Keller, J.L. Thoulence, and J. Flouquet, Solid State Commun. **85**, 355 (1993).
- <sup>18</sup>J.S. Brooks, R.V. Chamberlin, Y.P. Ma, and M.J. Naughton, Rev. Sci. Instrum. **58**, 117 (1987).
- <sup>19</sup>P.H. Frings and J.J. Franse, Phys. Rev. B **31**, 4355 (1985).
- <sup>20</sup>E. Schuberth, G. Hofmann, F. Gross, K. Andres, and J. Hufnagl, Europhys. Lett. **11**, 249 (1990).
- <sup>21</sup>A. Schenstrom, M.-F. Xu, Y. Hong, D. Bein, M. Levy, B.K. Sarma, S. Adenwalla, Z. Zhao, T. Tokuyasu, D.W. Hess, J.B. Ketterson, J.A. Sauls, and D.G. Hinks, Phys. Rev. Lett. **62**, 332 (1989).
- <sup>22</sup>E.I. Blount, C.M. Varma, and G. Aeppli, Phys. Rev. Lett. **64**, 3074 (1990).
- <sup>23</sup>K. Tenya, M. Ikeda, T. Tayama, T. Sakakibara, E. Yamamoto, K. Maezawa, N. Kimura, R. Settai, and Y. Onuki, Phys. Rev. Lett. **77**, 3193 (1996).
- <sup>24</sup>Brett Ellman and Louis Taillefer, Phys. Rev. B **56**, R5767 (1997).
- <sup>25</sup>P. Gegenwart, M. Deppe, M. Köppen, F. Kromer, M. Lang, R. Modler, M. Weiden, C. Geibel, F. Steglich, T. Fukase, and N. Toyota, Ann. Phys. (Leipzig) **5**, 307 (1996).
- <sup>26</sup>M. Tachiki, S. Takahashi, P. Gegenwart, M. Weiden, M. Lang, C. Geibel, F. Steglich, R. Modler, C. Paulsen, and Y. Onuki, Z. Phys. B: Condens. Matter **64**, 369 (1996).
- <sup>27</sup>P. Fulde and R.A. Ferrell, Phys. Rev. **135**, 550 (1964).
- <sup>28</sup>A.I. Larkin and Y.N. Ovchinnikov, Zh. Eksp. Teor. Fiz. **47**, 1136 (1964) [Sov. Phys. JETP **20**, 762 (1964)].
- <sup>29</sup>G. Bruls, D. Finsterbusch, I. Kouroudis, B. Wolf, D. Wichert, B. Lüthi, L. Jansen, and L. Taillefer, Physica B **223-224**, 36 (1996).
- <sup>30</sup>R. Joynt, Europhys. Lett. **16**, 289 (1991).
- <sup>31</sup>T.A. Tokuyasu, D.W. Hess, and J.A. Sauls, Phys. Rev. B **41**, 8891 (1990).
- <sup>32</sup>U. Yaron, P.L. Gammel, G.S. Boebinger, G. Aeppli, P. Schiffer, E. Bucher, D.J. Bishop, C. Broholm, and K. Mortensen, Phys. Rev. Lett. **78**, 3185 (1997).
- <sup>33</sup>R. Joynt, Phys. Rev. Lett. **78**, 3189 (1997).
- <sup>34</sup>G.R. Stewart, J. Appl. Phys. **57**, 3049 (1985).
- <sup>35</sup>G. Aeppli, E. Bucher, J. Baumann, and J. Hufnagl, Phys. Rev. Lett. **60**, 615 (1988).
- <sup>36</sup>Y. Koike, N. Metoki, N. Kimura, E. Yamamoto, Y. Haga, Y. Onuki, and K. Maezawa, J. Phys. Soc. Jpn. **67**, 1142 (1998).
- <sup>37</sup>I.A. Fomin and J. Flouquet, Solid State Commun. **98**, 795 (1996).
- <sup>38</sup>E. A. Schuberth, Int. J. Mod. Phys. B **10**, 357 (1996).